Spring International Engineering Research Journal: ISSN: 2384-5058

Volume-12 | Issue-4| April, Pp 17-30, 2024 |

Research Papers

Application of Response Surface Methodology in Predicting the Yield Strength as a Response in Mild Steel Weldment

[1]Emerahighe B., [1]Achebo J. I., [2]Obahiagbon K. O., *[1]Uwoghiren F. O.

[1]Department of Production Engineering, University of Benin, Benin City, +234, Nigeria.
[2]Department of Chemical Engineering, University of Benin, Benin City, +234, Nigeria.
E-mail:benetek2000@yahoo.co.uk,joseph.achebo@uniben.edu,kess.obahiagbon@uniben.edu,
*frank.uwoghiren@uniben.edu

Accepted: 12/4/2024|

Abstract: In any welding process, the weld's yield strength relative to the source metal is the most ideal strength parameter. The increasing need for stronger weld connections in structural and industrial materials necessitates a constant review and improvement of the welding process parameters. The relationship between certain mild steel weldment input variables (current, voltage, and gas flow rate) and their matching response variables has proven a problem. Response surface methodology (RSM) is used in this study to try to find a second-order logical link between the response variable (yield strength) and a subset of the input variables (current (I), voltage (V), and gas flow rate (GFR). In this study, we employed the Response Surface Methodology (RSM) for analysis, following the production of the central composite design matrix using the design expert program. This resulted in 20 experimental runs. Using the RSM and 170 amps of current, 18 volts of voltage, and 10.00 litres per minute of gas flow, we were able to get a mild steel weldment yield strength of 256.01. This study demonstrates that using the Response Surface Methodology (RSM) can improve the efficiency of TIG mild steel and forecast its yield strength.

Keywords: application, surface, yield strength, mild steel welding

Published:23/4/2024 2024.

1. INTRODUCTION

Welded structures, particularly those crafted from mild steel, often rely on optimal yield strength to ensure durability and reliability (Camacho et al., 2018). Yield strength is a fundamental mechanical property that dictates the material's ability to withstand deformation under applied stress (Samykano, 2021). Understanding and optimizing yield strength is critical for ensuring structural stability and longevity in the context of mild steel weldments (Voisin et al., 2021). This section delves into the complexities of yield strength and its implications in the welding industry.

Response Surface Methodology takes center stage as a systematic approach for modeling and optimizing the complex relationship between welding parameters and yield strength (Zhou et al., 2023). This segment elucidates the theoretical foundations of RSM, shedding light on how it becomes a guiding framework for achieving optimal yield strength in mild steel weldments (Marian and Tremmel, 2021). Strategies for optimWe explore strategies for optimizing yield strength in mild steel weldments, specifically focusing on using RSM to fine-tune welding parameters (Gunasekaran et al., 2023). w investigates how RSM aids in identifying optimal conditions that enhance yield strength while maintaining the structural integrity of the weldment (Senthil et al., 2020). Real-world applications and case studies exemplify successful optimisation strategies in diverse welding scenarios.

Yield strength is a fundamental mechanical property that plays a pivotal role in understanding how a material behaves under applied stress (Sabzi and Rivera-Daz-del-Castillo, 2020). Yield strength is defined as the level of stress at which a material undergoes significant plastic or permanent deformation without fracturing. It signifies the shift from elastic deformation, where the material regains its original shape after stress removal, to plastic deformation, where permanent changes take place (Hertzberg et al., 2020). Optimizing yield strength is paramount in welding, especially in structures crafted from mild steel. This mechanical property determines the material's ability to withstand deformation and stresses, ensuring the structural integrity and reliability of welded

components (Asprone et al., 2022). Understanding and fine-tuning yield strength are critical to achieving durable and high-performance weldments. Accurate prediction of yield strength is not without challenges. Variations in material properties, intricate welding processes, and computational complexities pose hurdles (Ansari et al., 2021).

The review candidly addresses the challenges associated with accurately predicting yield strength, taking into account factors such as current, voltage, and gas flow rate. It offers insights into how RSM serves as a predictive tool, bridging the gap between theoretical modelling and real-world outcomes in the realm of yield strength prediction (Basu et al., 2022). Real-world case studies and practical applications take prominence, illustrating the effectiveness of RSM in predicting and optimising yield strength in mild steel weldments. These examples serve as valuable narratives, highlighting the adaptability and success of RSM in diverse welding environments (Prabhakar et al., 2023). The literature review contemplates future research directions and potential innovations in the field of yield strength optimization. Future advancements in algorithmic efficiency, the integration of advanced materials, and the exploration of novel welding techniques are considered pathways for furthering the understanding and management of yield strength in mild steel weldments.

In conclusion, yield strength stands as a critical mechanical property, particularly in the welding domain, where structural integrity is paramount. The strategic application of Response Surface Methodology proves instrumental in navigating the complexities associated with yield strength, paving the way for enhanced weld integrity and performance in mild steel applications.

2.0 METHODOLOGY

2.1 Design of the experiment

In the modern optimisation process, experimental design plays a critical role. Previously, the process focused on one factor or variable at a time. Today, we employ an experiment design to collect data for appropriate polynomial selection. Experimental design follows the rules of repetition, randomization, and local control. Today, we employ an experiment design to collect data for appropriate polynomial selection. Experimental design follows the rules of repetition, randomization, and local control. The number of input parameters determines the form of experimental design; in this study, we chose the central composite design due to its superior ability to handle three inputs. Other types of experimental designs include Taguchi, D-optimal, factorial, and Latin hypercube designs

.2.2 Samples and sampling technique

After the edges were machined and bevelled, the plates were welded using tungsten inert gas welding equipment. Figure 1 depicts the setup for TIG welding

.

Figure 1: TIG equipment

In this research investigation, 100% pure argon gas was employed as the shielding gas during the welding process to protect the weld specimen from ambient interaction. The shielding gas regulator and cylinder are shown in Figure 2.

Figure 2: Shielding Gas Cylinder and Regulator

We created the weld samples from a mild steel plate with a thickness of 10 mm, trimming it to size with a power hacksaw. We polished the surfaces with emery paper, welded the joints, ground the edges, and measured and documented the results.

2.3 Method of Data Collection

We created the center composite design matrix using the design expert programme, which resulted in 20 experimental runs. The reactions observed in the weld samples served as data, while the input and output parameters comprised the experimental matrix.

2.4 Response Surface Methodology

Researchers frequently search for conditions that would optimize the process of interest. Stated differently, they seek to ascertain the process input parameter values at which the responses maximize. In terms of the process input parameters, the optimal value of a given function may be either minimum or maximum. RSM is one of the optimization techniques currently in widespread use to describe the welding process's performance and find the optimum of the responses of interest. RSM is a set of mathematical and statistical techniques that are useful for modelling and predicting the response of interest affected by several input variables with the aim of optimising this response.

2.5: Testing the adequacy of the models developed

We evaluated the effectiveness of the created models using the analysis of variance (ANOVA). We used the same software to analyse the generated models and every term in the regression equation to determine the best fit. The sequential F-test, lack-of-fit test, and other adequacy measures (such as R2, Adj-R~, Pred. R2, and Adeq. Precision ratio) were employed. We can utilize ANOVA to determine the model's probability >F, also referred to as the p-value, and the probability of each term within the model. If the probability of the model and each of its terms does not exceed the significance level (let's say a = 0.05), we can consider the model adequate within the confidence range of (1-a). The lack-of-fit test may deem the lack of fit insignificant if the probability of the lack of fit exceeds the significance level.

3. RESULTS AND DISCUSSION

3.1 Modelling and Optimisation using RSM

Response surface methodology (RSM) is used in this study to try and find a second-order logical relationship between the response variable (yield strength) and certain input variables (current (I), voltage (V), and gas flow rate (GFR)).

The ultimate goal of the optimisation process was to ascertain the ideal value of each input variable, specifically the current (Amp), voltage (Volt), and gas flow rate (l/min), in order to optimise output intensity. This was the optimisation model's purpose.

To obtain the empirical information required for the optimization method,

7. Initially, we utilized the central composite design approach (CCD) to finalize the statistical design of the experiment. A statistical tool was used to carry out the design and optimization. We used Design Expert 7.01 in this specific case.
8. Second, we created an experimental design matrix that yielded 20 experimental runs with six (6)

centre points (k), six (6) axial points (2n), and eight (8) factorial points (2n).

As shown in Table 1, we computed the sequential model sum of squares for the yield strength response to con

firm that the quadratic model was suitable for interpreting the experimental data.

Table 1: Sequential model sum of square for yield strength

Source	Sum of Squares	df	Mean Square	F Value	p-value Prob > F	
Mean vs Total	1.064E+006	1	1.064E+006			
Linear vs Mean	3585.17	3	1195.06	3.17	0.0529	
2FI vs Linear	784.38	3	261.46	0.65	0.5978	
Quadratic vs 2FI	4938.45	3	1646.15	54.11	< 0.0001	Suggested
Cubic vs Quadratic	204.83	4	51.21	3.09	0.1053	Aliased
Residual	99.38	6	16.56			
Total	1.074E+006	20	53703.10			

The sequential model sum of squares table displays the cumulative improvement in the model fit as term additions occur. Based on the sequential model's computed sum of squares, we selected the highest-order polynomial as the best fit, where the extra terms are significant and the model remains aliased. Table 1's data aliased the cubic polynomial, preventing its use in fitting the final modFurthermore, we suggested that the quadratic and 2FI models best fit the data, thereby supporting the use of quadratic polynomials in this analysis.sis.

We estimated the lack of fit test for each response to assess how well the quadratic equation model could explain the inherent variance in the experimental data. For prediction, it is impossible to use a model with a significant lack of fit.

Table 2 displays the results of the calculated yield strength deficienc

Table 2: Lack of fit test for yield strength

Source	Sum of Squares	Df	Mean Square	F Value	p-value Prob > F	
Linear	6027.03	11	547.91	7.11	0.0211	
2FI	5242.66	8	655.33	9.41	0.0122	
Quadratic	304.21	5	60.84	0.70	0.6456	Suggested
Cubic	99.38	1	99.38	0.22	0.6561	Aliased
Pure Error	0.000	5	0.000			

Table 2's results confirmed that the cubic polynomial had a substantial lack of fit and was therefore aliased to model analysis, whereas the quadratic polynomial had a non-significant lack of fit and was suggested for model analysis.

Table 3 displays the model statistics that were calculated for the yield strength response using the model sources.

Table 3: Model summary statistics for yield strength

Source	Std. Dev.	R-Squared	Adjusted R-Squared	Predicted R-Squared	PRESS	
Linear	19.41	0.3730	0.2554	0.0387	9240.02	
2FI	20.08	0.4546	0.2029	-0.6059	15436.52	
Quadratic	5.52	0.9684	0.9399	0.7473	2428.93	Suggested
Cubic	4.07	0.9897	0.9673	-1.2790	21905.90	Aliased

For every entire model, the standard deviation, r-squared, adjusted r-squared, predicted r-squared, and predicted error sum of squares (PRESS) statistics are displayed in the summary statistics of model fit. The ideal criteria for selecting the optimal model source are a low standard deviation, an R-squared close to one, and a reasonably low PRESS. Table 3's results advised aliasing the cubic polynomial model, leading to the use of the quadratic polynomial model in this study.

Table 4 displays the one-way analysis of variance (ANOVA) table that was created for the yield strength in order to evaluate the quadratic model's strength..

Table 4: ANOVA table for yield strength

Source	Sum of Squares	Df	Mean Square	F Value	p-value Prob > F	
Model	9307.99	9	1034.22	34.00	< 0.0001	Significant
A-current	3413.38	1	3413.38	112.21	< 0.0001	
B-voltage	68.32	1	68.32	2.25	0.1649	
C-gas flow rate	103.47	1	103.47	3.40	0.0949	
AB	703.13	1	703.13	23.11	0.0007	
AC	66.12	1	66.12	2.17	0.1712	
BC	15.13	1	15.13	0.50	0.4968	
A^2	1445.73	1	1445.73	47.52	< 0.0001	
B^2	3866.58	1	3866.58	127.10	< 0.0001	
C^2	252.08	1	252.08	8.29	0.0164	
Residual	304.21	10	30.42			
Lack of fit	304.21	5	60.84	0.70	0.6456	not significant
Pure Error	0.000	5	0.000			
Cor Total	9612.20	19				

To determine whether the model is significant and assess the substantial contributions of every distinct parameter, the combined effects, and the quadratic effects towards each answer, an analysis of variance (ANOVA) was required. According to Table 4's results, the model's 34.00 model F-value suggests that it is significant. Noise has a mere 0.01% probability of producing a "model F-value" of this magnitude. "Prob > F" values less than 0.0500 suggest the significance of the model terms. In this case, A, B, AB, BC, A2, B2, and C2 are important model terms. If the value is greater than 0.1000, the model terms are not important. The "Lack of Fit F-value" of 0.70 indicates that, in comparison to the pure error, the lack of fit is not significant. A significant "Lack of Fit F-value" has a 64.56% probability of being caused by noise. A non-significant lack of fit suggests a significant model, which is excellent.

Table 5 displays the yield strength and goodness of fit statistics to verify the quadratic model's suitability

.

Table 5: Goodness of fit statistics for yield strength

Std. Dev.	5.52	R-Squared	0.9684
Mean	230.70	Adj R-Squared	0.9399
C.V. %	2.39	Pred R-Squared	0.7473
PRESS	2428.93	Adeq Precision	14.815

Figure 5's result showed that there is a decent amount of agreement between the "Adj R-Squared" value of 0.9399 and the "Predicted R-Squared" value of 0.7473. The signal to noise ratio is measured with adequate precision. Ideally, the ratio should be higher than 4. Table 5's computed ratio of 14.815 suggests that the signal is sufficient. With the aid of this model, one can effectively explore the design space and forecast the yield strength.

We initially take into account the coefficient statistics and the associated standard errors in order to get the best solution. The difference between the experimental terms and their corresponding anticipated terms is measured by the computed standard error.

Table 6 displays yield strength coefficient statistics.

Table 6: Coefficient estimates statistics generated for yield stength

	Coefficient		Standard	95% CI	95% CI	
Intercept	209.82	1	2.25	204.81	214.83	
A-current	15.81	1	1.49	12.48	19.13	1.00
B-voltage	-2.24	1	1.49	-5.56	1.09	1.00
C-gas flow rate	-2.75	1	1.49	-6.08	0.57	1.00
AB	9.38	1	1.95	5.03	13.72	1.00
AC	-2.87	1	1.95	-7.22	1.47	1.00
BC	1.38	1	1.95	-2.97	5.72	1.00
A^2	10.02	1	1.45	6.78	13.25	1.02
B^2	16.38	1	1.45	13.14	19.62	1.02
C^2	4.18	1	1.45	0.95	7.42	1.02

Based on the coded data, the ideal equation is supplied that illustrates the combined interactions and individual effects of the chosen input variables (current, voltage, and gas flow rate) versus the measured yield strength.

Final Equation in Terms of Coded Factors:

$$\begin{aligned} \text{yield strength} = {} & \\ & +209.82 \\ & +15.81 * A \\ & -2.24 * B \\ & -2.75 * C \\ & +9.38 * A * B \\ & -2.87 * A * C \\ & +1.38 * B * C \\ & +10.02 * A^2 \\ & +16.38 * B^2 \\ & +4.18 * C^2 \end{aligned}$$

The optimal equation which shows the individual effects and combine interactions of the selected input variables (current, voltage and gas flow rate) against the mesured yield strength is presented based on the actual values.

Final Equation in Terms of Actual Factors:

yield strength =
+5348.80391
-19.40136 * current
-357.02085 * voltage
-36.69883 * gas flow rate
+0.41667 * current * voltage
-0.12778 * current * gas flow rate
+0.61111 * voltage * gas flow rate
+0.044515 * current^2
+7.27997 * voltage^2
+1.85881 * gas flow rate^2

Table 7 presents the diagnostics case statistics, which compare the observed yield strength values to their expected values. In fact, the diagnostic case statistics shed light on the suitability of the ideal second-order polynomial equation as well as the strength of the model.

Table 7: Diagnostics case statistics report of observed versus predicted yield strength

Standard Order	Actual Value	Predicted Value	Residual	Leverage	Studentized Residual	Studentized Residual	Fitted Value DFFITS	Cook's Distance	Run Order
1	235.00	237.45	-2.45	0.670	-0.774	-0.757	-1.078	0.121	14
2	257.00	256.07	0.93	0.670	0.293	0.279	0.397	0.017	2
3	218.00	211.48	6.52	0.670	2.057	2.570	* 3.66	0.858	16
4	265.00	267.60	-2.60	0.670	-0.820	-0.805	-1.147	0.136	9
5	242.00	234.95	7.05	0.670	2.225	2.971	* 4.23	* 1.00	7
6	240.00	242.07	-2.07	0.670	-0.652	-0.632	-0.900	0.086	15
7	218.00	214.47	3.53	0.670	1.112	1.127	1.605	0.251	20
8	266.00	259.09	6.91	0.670	2.179	2.853	* 4.06	0.963	1
9	205.00	211.56	-6.56	0.607	-1.898	-2.252	* -2.80	0.557	11
10	265.00	264.74	0.26	0.607	0.076	0.072	0.090	0.001	6
11	260.00	259.91	0.089	0.607	0.026	0.024	0.030	0.000	3
12	246.00	252.39	-6.39	0.607	-1.848	-2.161	* -2.69	0.528	10
13	227.00	226.28	0.72	0.607	0.209	0.198	0.247	0.007	4
14	210.00	217.02	-7.02	0.607	-2.031	-2.514	* -3.13	0.638	8
15	210.00	209.82	0.18	0.166	0.036	0.034	0.015	0.000	5
16	210.00	209.82	0.18	0.166	0.036	0.034	0.015	0.000	19
17	210.00	209.82	0.18	0.166	0.036	0.034	0.015	0.000	18
18	210.00	209.82	0.18	0.166	0.036	0.034	0.015	0.000	13
19	210.00	209.82	0.18	0.166	0.036	0.034	0.015	0.000	12
20	210.00	209.82	0.18	0.166	0.036	0.034	0.015	0.000	17

Any model's acceptability must first be verified by the results of a suitable statistical study. The response surface model's statistical characteristics can be diagnosed using the residual normal probability plot shown in Figure 3.

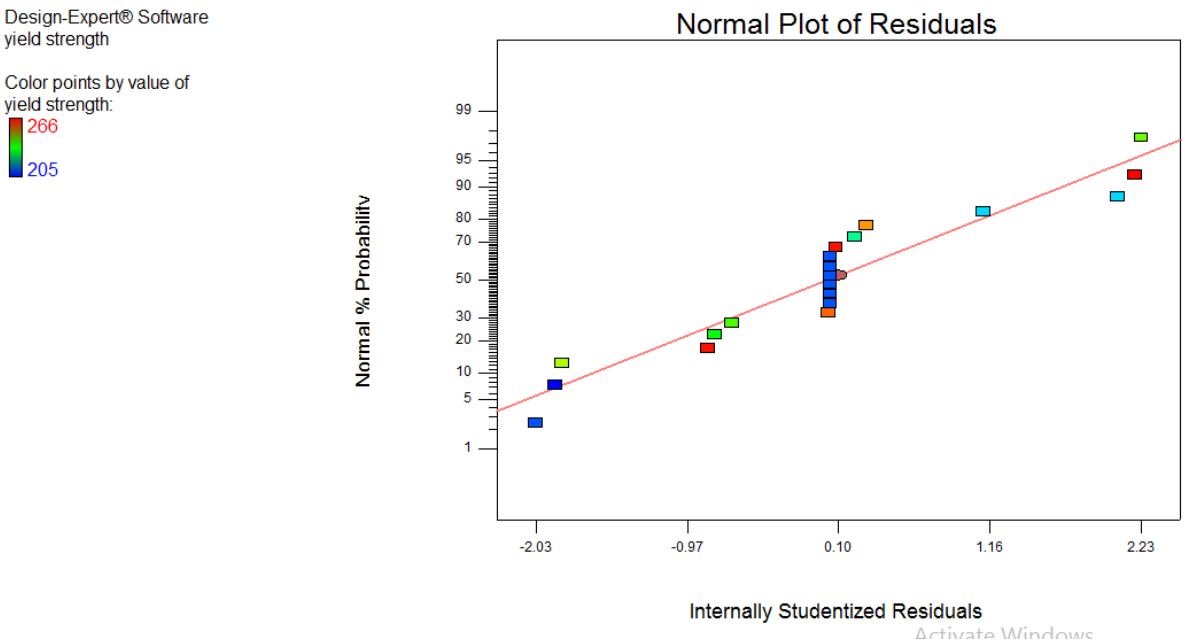

Figure 3: Normal probability plot of studentized residuals for Yield strength

Despite the modest spread, it is evident that the points follow a straight line. Aside from the linear trend, there is no discernible pattern, such as an "s-shaped" curve. This suggests that the residuals follow a normal distribution and that further processing of the response data is not necessary for a more accurate interpretation. We used the normal probability plot of studentized residuals to evaluate the normality of the computed residuals. We used the normal probability plot of residuals, which is the number of standard deviations of actual values based on the projected values, to determine if the residuals (observed and expected) follow a normal distribution. It is the most important presumption for determining whether a statistical model is adequate. The estimated residuals in Figure 3 are roughly normally distributed, indicating that the constructed model is satisfactory.

Figure 4 displays the predicted yield strength after producing a plot of residuals to identify the presence of mega patterns or expanding variance.

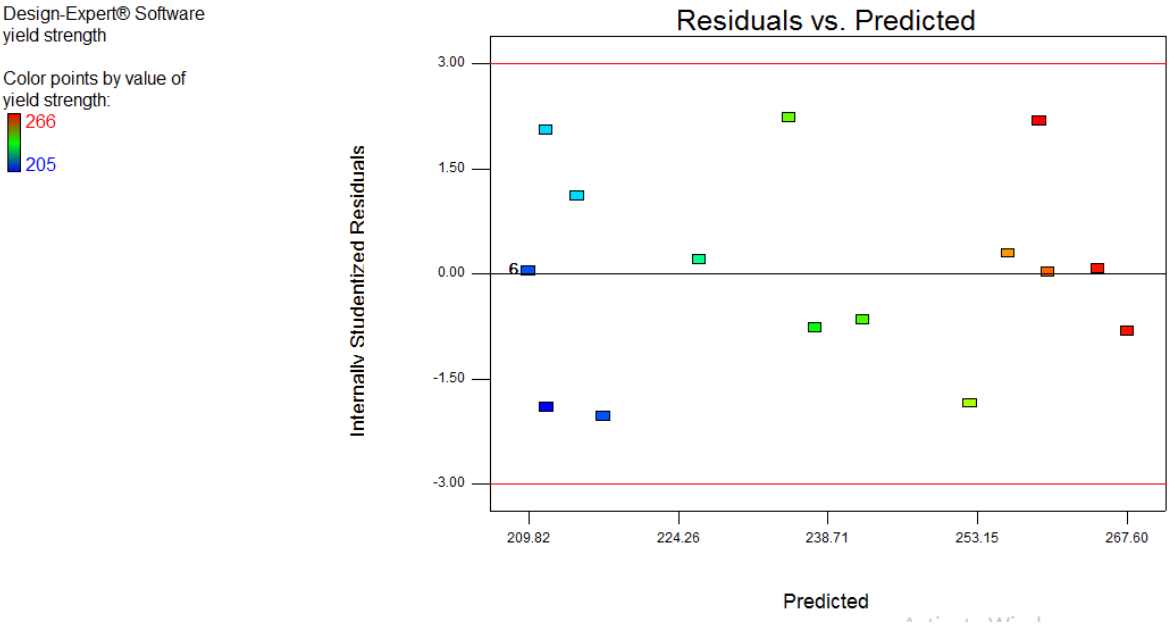

Figure 4: Plot of Residual vs Predicted for yield strength

The graph shows that the spots are in close proximity to the line of fit. For the most part, the model can accurately anticipate the data points.

For yield strength, which is depicted in figure 5, the predicted values are compared to the actual values in order to identify a value or set of values that the model is unable to identify with ease.

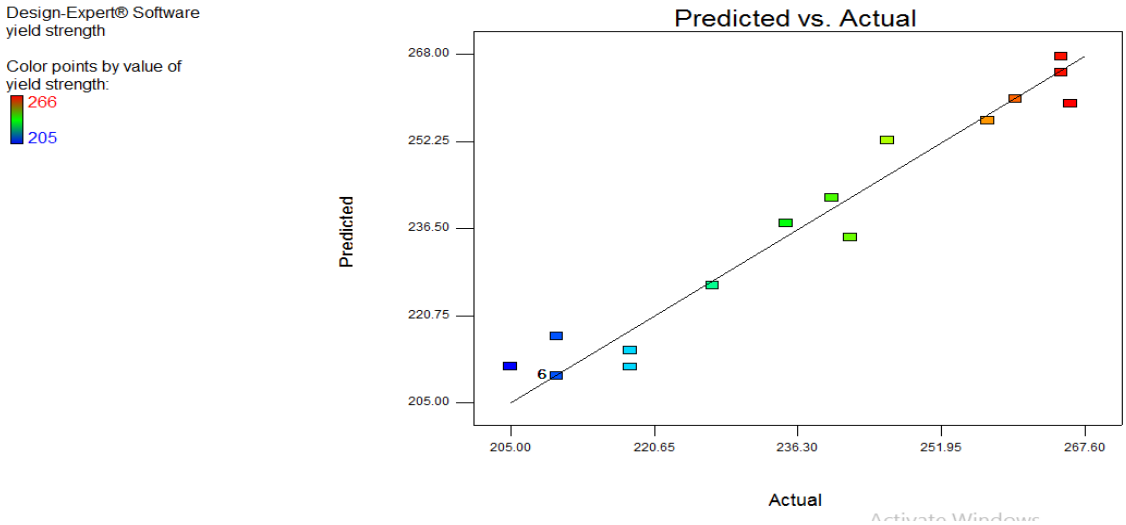

Figure 5: Plot of Predicted Vs Actual for Yield strength

To measure the influence of each data point of yield strength on the predicted value a Plot of DFFITS Vs Run was produce shown in the figure 6.

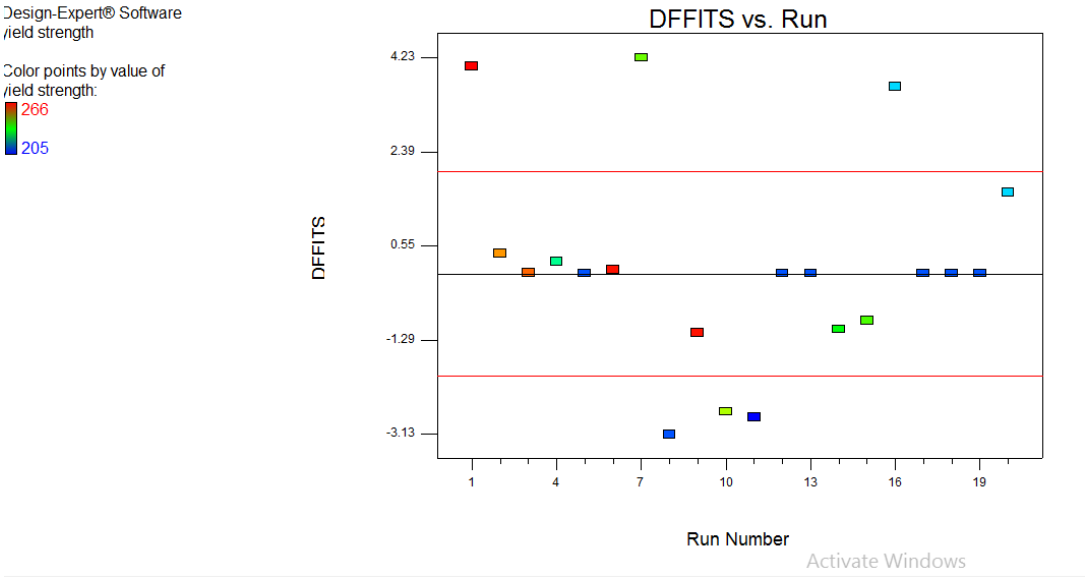

Figure 6: Plot of DFFITS Vs Run s yield strength

DFFITS vs run plot is a visual tool that represents the degree to which the ith observation affects the value that is expected. It is better to have lower values. Keep an eye out for spots that go over the estimated bounds.

The cook's distance plot was created for each response to ascertain whether the experimental data contained a potential anomaly. The amount that the regression would alter if the anomaly were removed from the study is shown by the cook's distance. It's important to look into any point that appears to be an anomaly and has a very high distance value in comparison to the other points. Figures 7 exhibit the generated cook's distance for the yield strength.

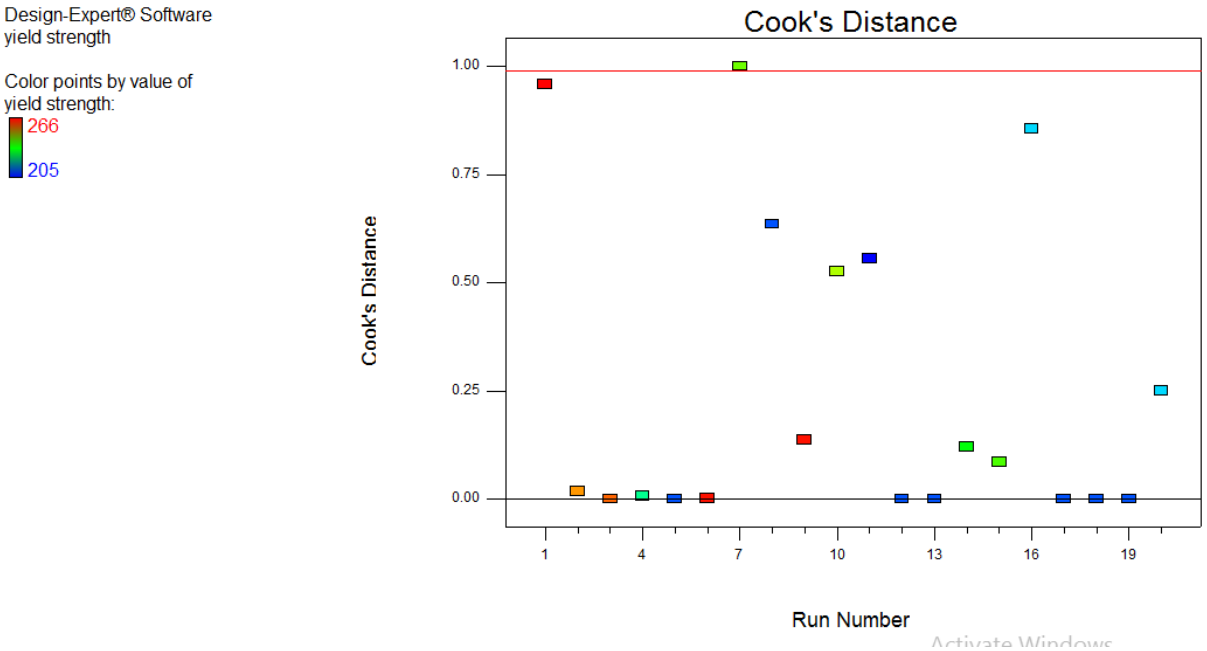

Figure 7: Generated cook's distance for yield strength

The lowest bound of the cook's distance plot is 0.00, and the upper bound is 1.00. The outliers are experimental values that fall outside of the lower or upper boundaries and need to be thoroughly examined. The results of Figure 7 show that there are no potential outliers in the data utilized for this analysis, demonstrating the suitability of the experimental data.

In order to investigate the impact of combining input variables on the yield strength, the 3D surface plots shown in Figure 8 were created using the following method:

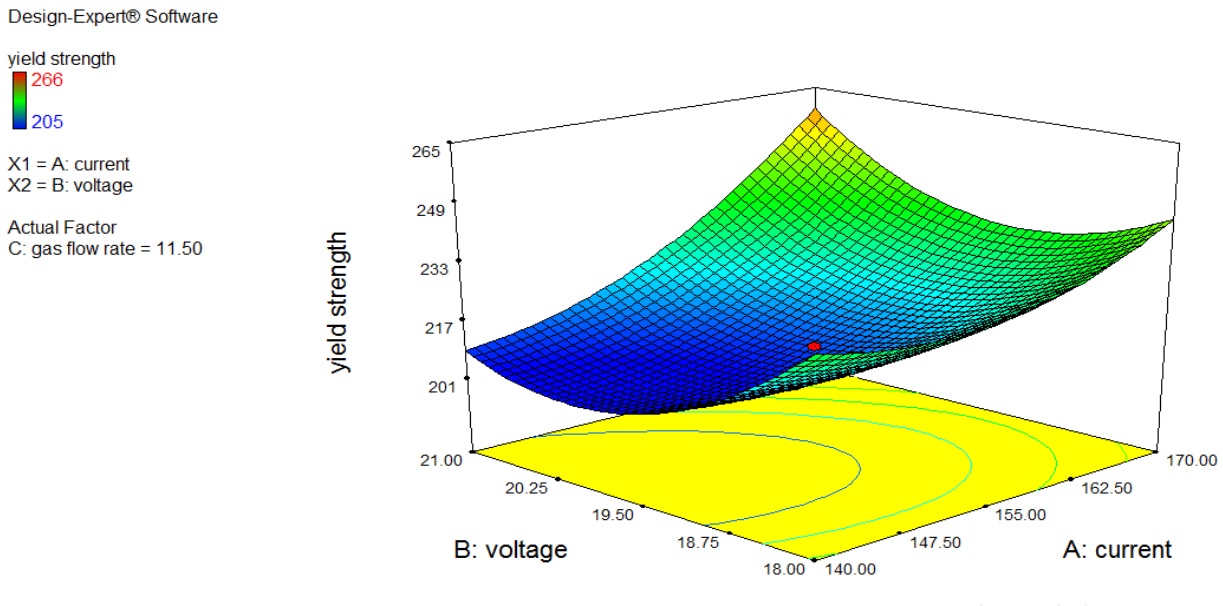

Figure 8: Effect of current and voltage on yield strength

In order to investigate the impact of combining input variables on the yield strength, the 3D surface plots shown in Figure 9 were created using the following method:

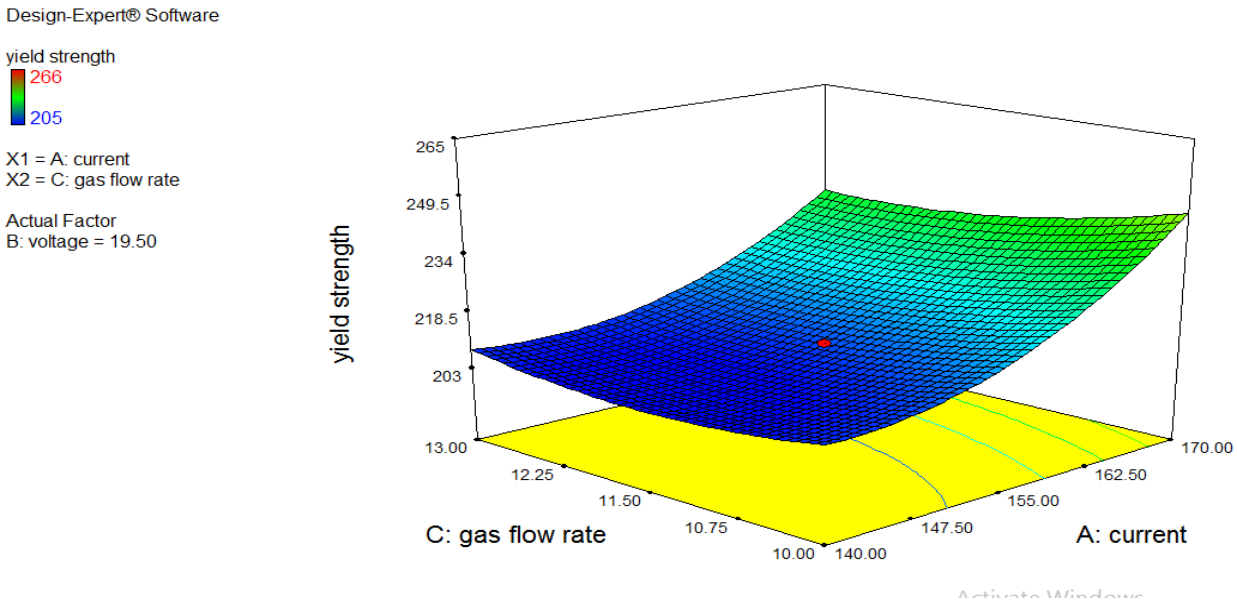

Figure 9: Effect of gas flow rate and current on yield strength

In order to investigate how combining input factors affects the yield strength, the 3D surface plots shown in Figure 10 were created using the following method:

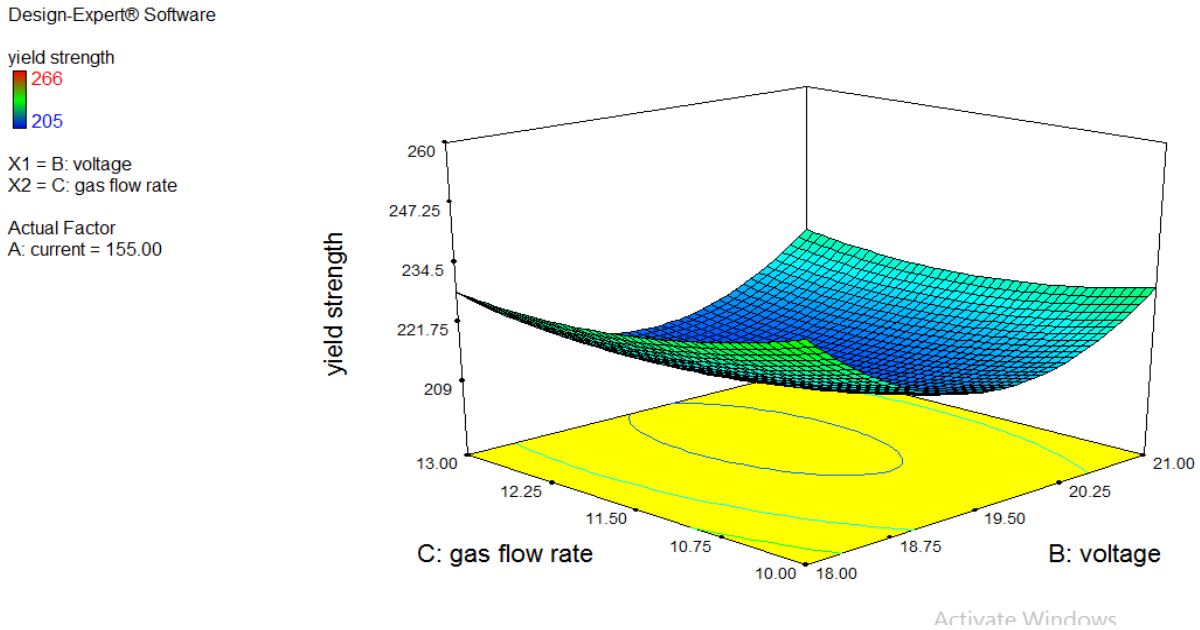

Figure 10: Impact of gas flow rate and voltage on yield strength

The link between the response variables (yield strength) and the input variables (current and voltage) is depicted in Figure 8's 3D surface plot. This three-dimensional surface graphic was used to help visualize the response surface. This image might give you a better idea of the surface, but it's not as helpful for determining

response values and coordinates as the contour plot is. The yield strength reduces correspondingly with increasing curve surface color. More points that were slightly tinted for simpler identification sank below the surface, as shown by the presence of a colored hole in the center of the upper surface.

It can be seen from the surface plot in Figure 9 that the surface's color lightens with increasing voltage and current. It follows that an increase in voltage and current will result in a corresponding rise in response value. Figure 10 shows that when gas flow rate and voltage increase, the surface's color becomes lighter.

Lastly, Figure 11 displays the contour plots of the yield strength response variable against the optimized value of current and voltage based on the optimal solution.

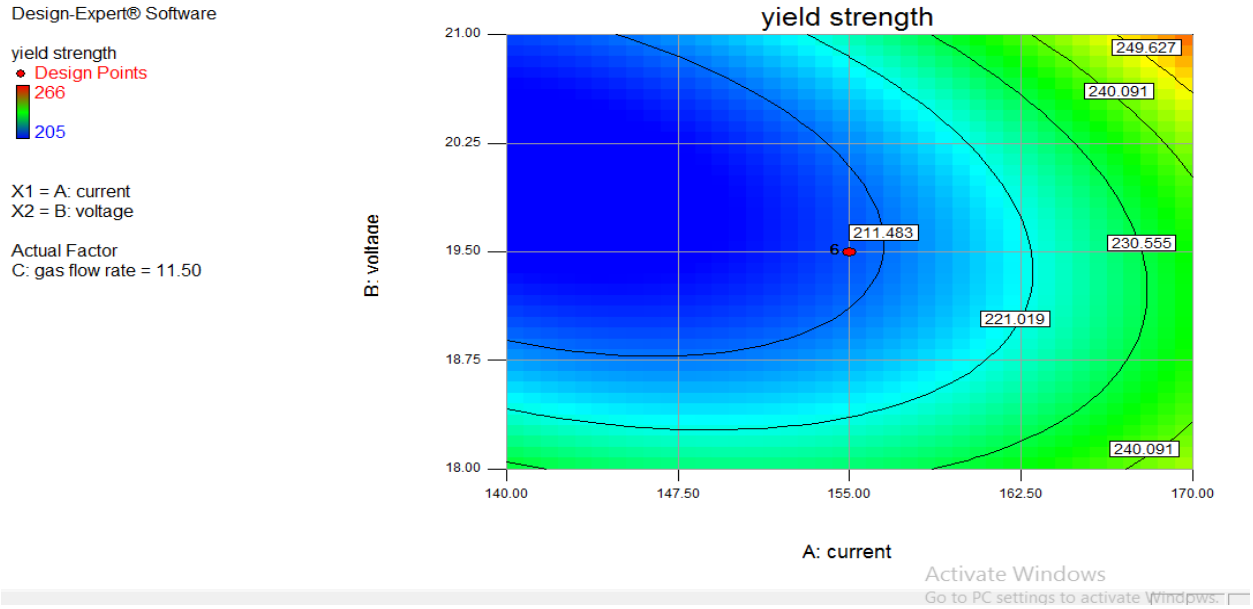

Figure 11: Predicting yield strength using contour plot

Figure 12 displays the contour plots that display the yield strength response variable against the gas flow rate and current optimized values.

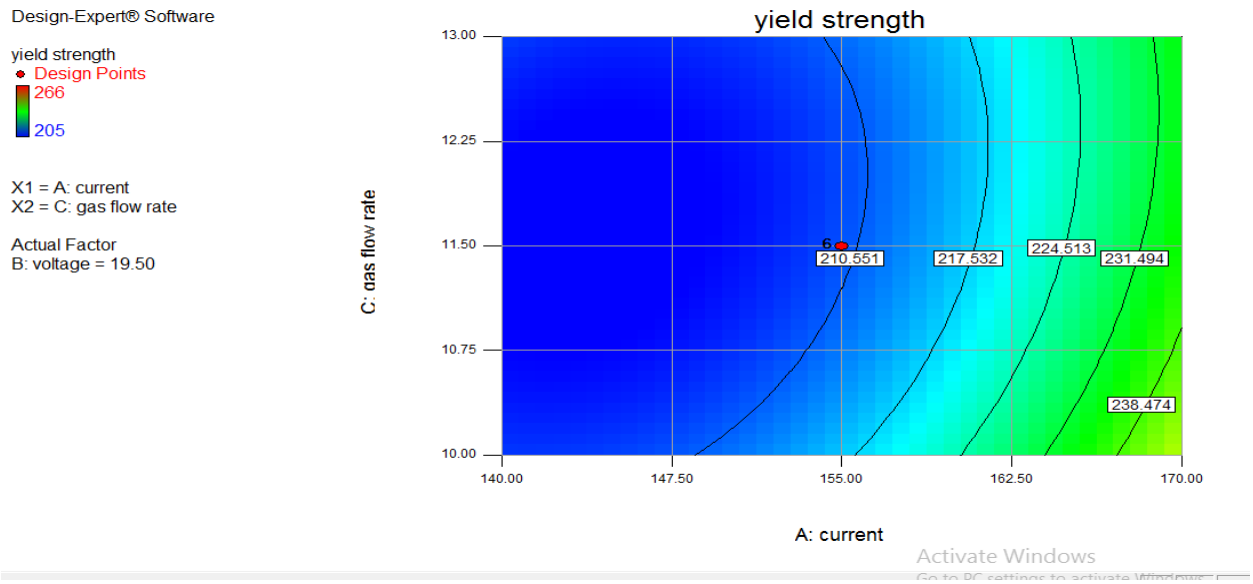

Figure 12: Predicting yield strength using contour plot

Figure 13 displays the contour plots that display the yield strength response variable against the gas flow rate and voltage optimum values.

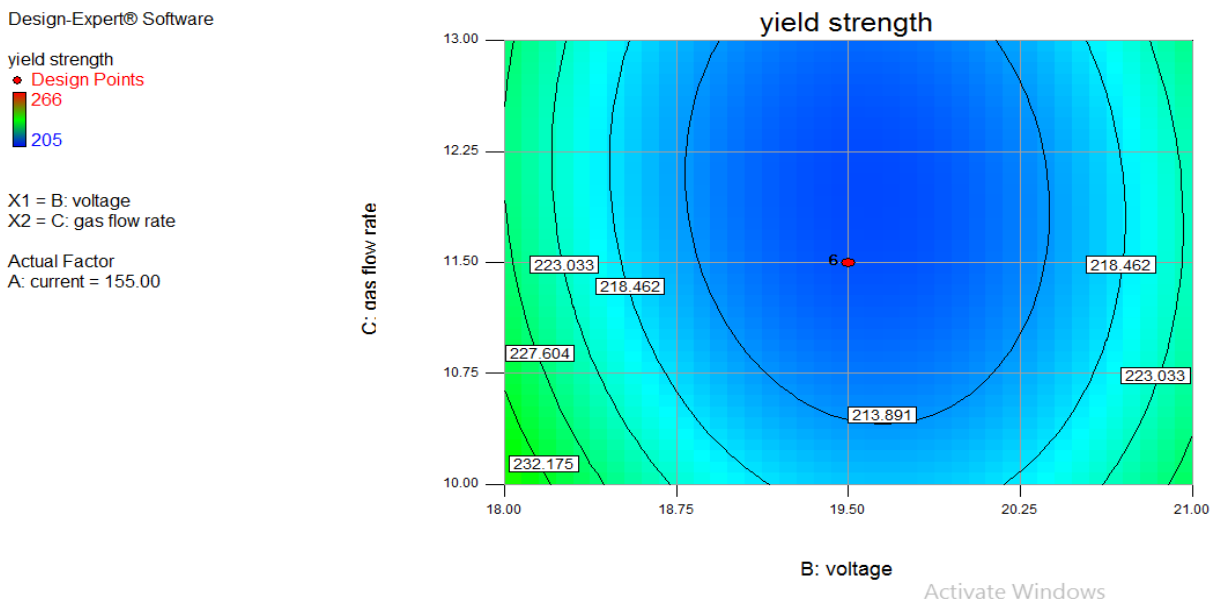

Figure 13: Predicting yield strength using contour plot

4. CONCLUSION

The implementation of response surface methodology to maximize yield strength has been demonstrated by the study. An 18 volt voltage, 170 amp current, and 10.00 l/min of gas flow rate will provide a welding process with a 256.01 yield strength. It has been successfully demonstrated that response surface methodology (RSM) can be applied to the central composite design approach for the purpose of optimizing and predicting the yield strength of TIG mild steel welds. The study's findings demonstrate that the RSM is a very useful tool for forecasting and optimizing the output reactions of TIG mild steel welds.

REFERENCES

1. Camacho, D. D., Clayton, P., O'Brien, W. J., Seepersad, C., Juenger, M., Ferron, R., & Salamone, S. (2018). Applications of additive manufacturing in the construction industry–A forward-looking review. *Automation in construction*, *89*, 110-119.

2. Samykano, M. (2021). Mechanical property and prediction model for FDM-3D printed polylactic acid (PLA). *Arabian Journal for Science and Engineering*, *46*, 7875-7892.

3. Voisin, T., Forien, J.B., Perron, A., Aubry, S., Bertin, N., Samanta, A., Baker, A. and Wang, Y.M., (2021). New insights on cellular structures strengthening mechanisms and thermal stability of an austenitic stainless steel fabricated by laser powder-bed-fusion. *Acta Materialia*, *203*, p.116476.

4. Zhou, D., Su, X., Yang, C., Kang, Z., & Li, Z. (2023). A systematic approach to model and optimize qualities of castings produced by squeeze casting process. *International Journal of Metalcasting*, *17*(3), 1715-1735.

5. Marian, M., and Tremmel, S. (2021). Current trends and applications of machine learning in tribology—a review. *Lubricants*, *9*(9), 86.

6. Gunasekaran, J., Sevvel, P., Roy, J. V., & Sivaramakrishnan, A. (2023). Analysis of sensitivity and formulation of empirical relationship between parameters of FSW process and tensile strength of AZ80A Mg alloy joints. *Materials Research Express*, *10*(5), 056513.

7. Senthil, S. M., Parameshwaran, R., Ragu Nathan, S., Bhuvanesh Kumar, M., & Deepandurai, K. (2020). A multi-objective optimization of the friction stir welding process using RSM-based-desirability function approach for joining aluminum alloy 6063-T6 pipes. *Structural and Multidisciplinary Optimization*, *62*, 1117-1133.

8. Basu, B., Gowtham, N. H., Xiao, Y., Kalidindi, S. R., & Leong, K. W. (2022). Biomaterialomics: Data science-driven pathways to develop fourth-generation biomaterials. *Acta Biomaterialia*, *143*, 1-25.

9. Prabhakar, D. A. P., Korgal, A., Shettigar, A. K., Herbert, M. A., Chandrashekharappa, M. P. G., Pimenov, D. Y., & Giasin, K. (2023). A Review of Optimization and Measurement Techniques of the Friction Stir Welding (FSW) Process. *Journal of Manufacturing and Materials Processing*, *7*(5), 181.

10. Sabzi, H. E., and Rivera-Díaz-del-Castillo, P. E. (2020). Composition and process parameter dependence of yield strength in laser powder bed fusion alloys. *Materials & Design*, *195*, 109024.

11. Hertzberg, R. W., Vinci, R. P., & Hertzberg, J. L. (2020). *Deformation and fracture mechanics of engineering materials*. John Wiley & Sons.

12. Asprone, D., Menna, C., Bos, F., Mata-Falcón, J., Ferrara, L., Auricchio, F., Cadoni, E., Cunha, V.M., Esposito, L., Fromm, A. and Grünewald, S., (2022). Structural design and testing of digitally manufactured concrete structures. *Digital Fabrication with Cement-Based Materials: State-of-the-Art Report of the RILEM TC 276-DFC*, pp.187-222.

13. Ansari, M., Jabari, E., & Toyserkani, E. (2021). Opportunities and challenges in additive manufacturing of functionally graded metallic materials via powder-fed laser directed energy deposition: A review. *Journal of Materials Processing Technology*, *294*, 117117.